APPENDIX J

RSDYK2008 –CORRELATION BETWEEN REMOTELY SENSED IMAGES AND 2-D ELECTRICAL IMAGING

Contents

1 ESTABLISHING CORRELATION BETWEEN REMOTELY SENSED IMAGES AND 2-D ELECTRICAL IMAGING

In this appendix is tried to establish the correlation between 2-D electrical imaging results and the thermal infrared (TIR) images as well as the correlation between the TIR and near infrared (NIR) of all seasons will be evaluated.

1.1 Analyzing the correlation between TIR images and 2-D electrical imaging results

The 2-D pseudo-section of the resistivity survey describes the vertical inclination (direct depth) of the dyke while the TIR images give more information on the top inclined surface of the dyke. The 2-D electrical imaging survey gives an apparent 2D section of the variation of the resistivity, but in reality measures the resistivity over a volume, thus also including variations perpendicular to the section. Therefore, even if the images of the two techniques show different parts of the dyke, it is possible to establish their relationship. The possible correlation was described for each site below. The sketch below shows the survey area covered by these techniques (Figure 1).

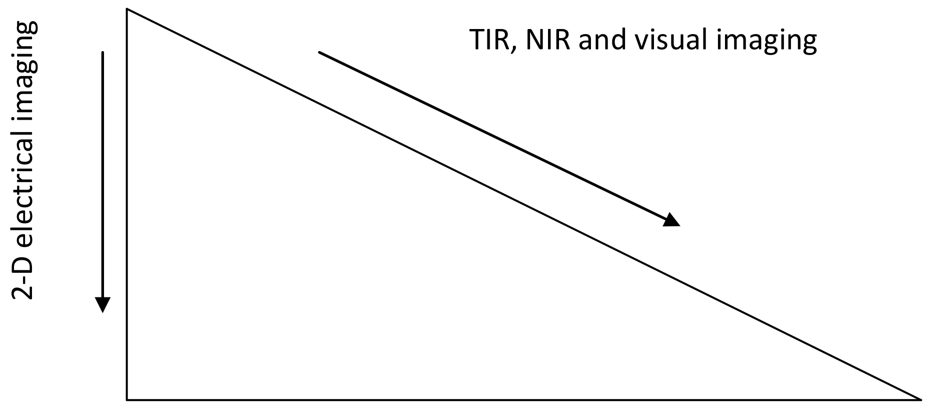

Figure 1. This sketch of the dyke shows the view of the 2-D electrical imaging survey in the vertical and the terrestrial remote sensing imaging (TIR, NIR and visual images) on the inclined surface of the dyke

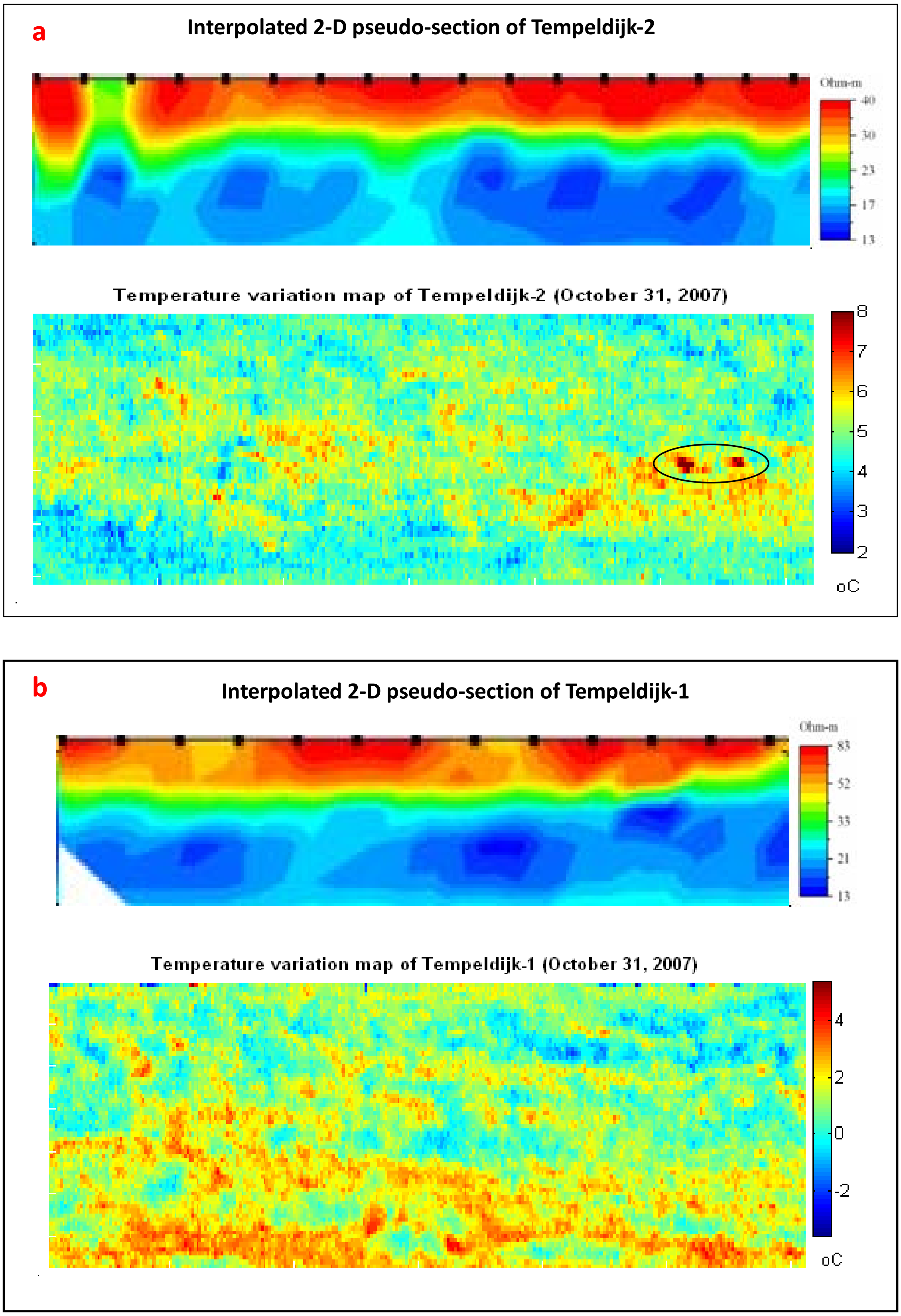

Figure 2. This figure shows the interpolated 2-D electrical imaging pseudo-sections and the thermal images of (a) Tempeldijk-South (the dark spot inside the circle indicates the exposed topsoil) and (b) Tempeldijk-North which were acquired in October 31, 2007 (Tempeldijk-1 is Tempeldijk-North and Tempeldijk-2 is Tempeldijk-South).

1.1.1 TEMPELDIJK-SOUTH

The sampled thermal image of the Tempeldijk-South covers a 10 X 16 m^2 area, which should be related to the 2.5 to 3 m depth information that is provided by the 2-D electrical imaging. The low radiation temperature on the top of the TIR image can be related to the higher resistivity value in the pseudo-section (Figure 2a). However, the low temperature at the bottom of the TIR image is mapped by low resistivity value. Apart from the compositional variation, this can be related to the accumulation of water depending on the steepness of the dyke. Possibly the bottom part has higher probability to accumulate more water than the middle part even they are considered as the same media. The low resistivity zone, which is mapped by the 2-D electrical imaging, is again the higher in magnitude of the thermal radiation in the middle part of the TIR image.

In order to examine the magnitude of the correlation, scatter plots are made between the resistivity survey result (conducted in October) and the thermal images of all periods (Figure 3). The 10 m inclination distance of the thermal images was projected to the 3m depth information of the resistivity survey.

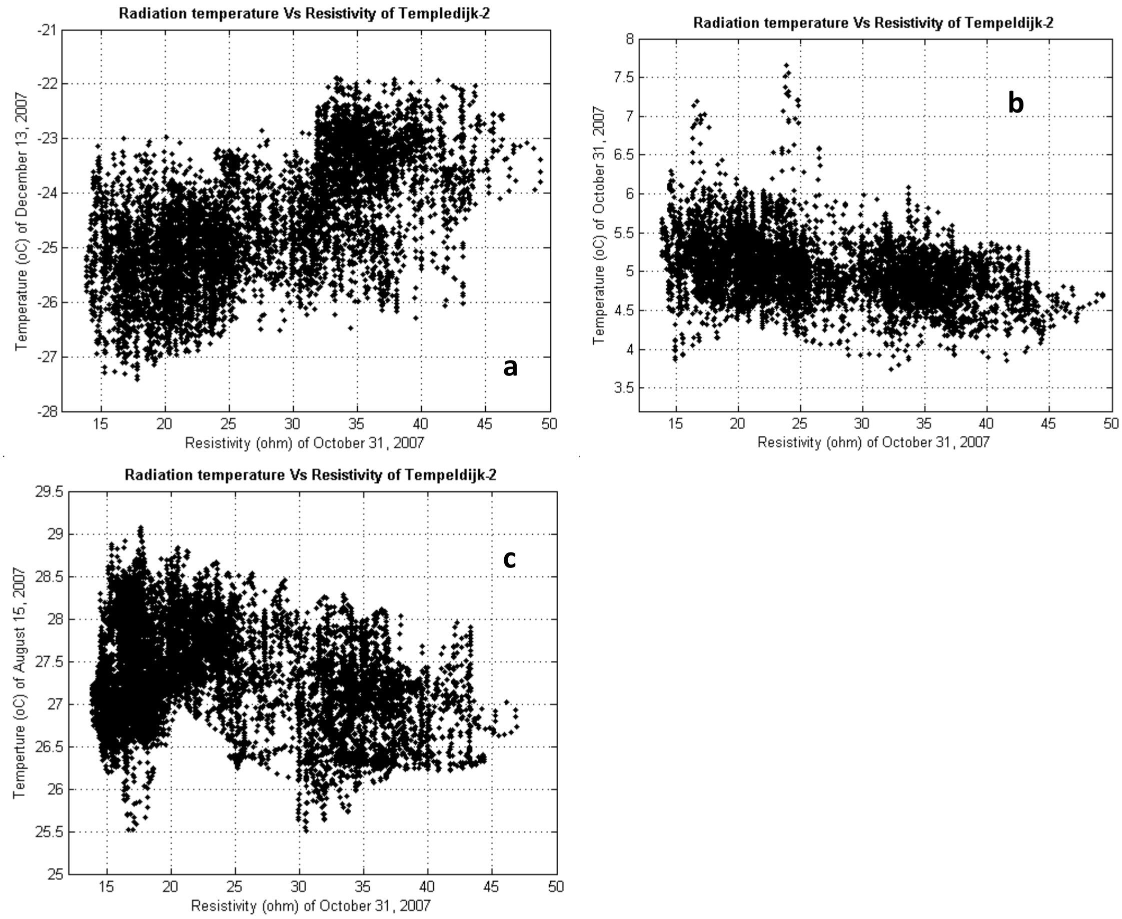

Figure 3. Scatter plot showing the possible correlation of resistivity conducted in October verses TIR images in (a) December, (b) October and (c) August of Tempeldijk-2

The plots show an overview on the general trend of the correlation (Figure 3). The thermal images of August as well as October show a negative relation with the resistivity. The negative correlation is relatively stronger with the TIR image of August than with the TIR image of October. However, the plot of the resistivity verses the TIR image of December shows a positive correlation. In the presence of water content, both techniques give relatively lower values than the surrounding area. However, these images indicate the differences are more than the similarities. This is because the radiation temperature values are mainly determined by the top layer of the dyke. , so the water with in the top layer can be easily reduce due to evaporation and evapo-transpiration especially in the dry season. The dryness of the peat became high in the summer while in December the top surface of the peat layer becomes wetter than the surrounding. These relations might be related to the subsurface of the dyke.

1.1.2 TEMPELDIJK-NORTH

The thermal image used for correlation has the same dimension as the image for Tempeldijk-South. The higher resistivity in the pseudo-section, which was classified as clay is mapped by a relatively low radiation temperature in the TIR image (Figure 2b). In the TIR image, this part was identified as wet and relatively cold area. The lower part of the images indicates a possible area of overlap between the lower resistivity and the higher magnitude of the emitted temperature. This part of the pseudo-section was classified as a peat layer with possibly high moisture content than the clay layer. However, the value of the radiation temperature of this layer shows that the area is relatively dry and warm. The middle layer in the pseudo-section (in green with 28 to 40ohm) is also not clearly mapped by the TIR. The lower temperature in the upper right side of the TIR image is possibly correlated with the higher resistivity value. This continues to the upper left side with some increment in radiation temperature that can also be observed as a lateral variation in the pseudo-section. The scatter plot illustrates the weak negative relationship between resistivity and the thermal radiation of the dyke in October (Figure 4). The general trend of the plot seems from the upper left corner (high temperature and low resistivity) to the lower right corner (relatively low temperature and high resistivity).

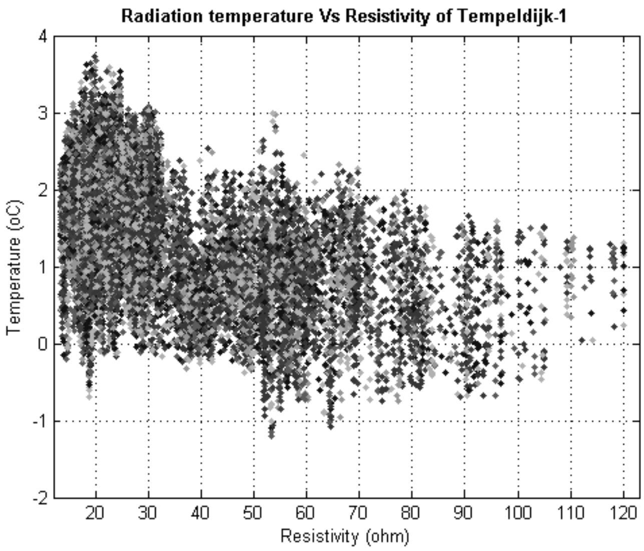

Figure 4. Scatter plot of resistivity verses thermal image of October for Tempeldijk-North (Tempeldijk-1 is Tempeldijk-South).

1.1.3 GENERAL EVALUATION

In both the TIR images, the vertical variation between the clay and the peat is not clear as they are mapped by the 2-D electrical imaging. From the thermal infrared and electrical imaging, it is clear to observe the indication in the low emissivity and high resistive response of the clay material. This might show that the increase in the temperature of the peat material inside. The spatial distribution of the emitted temperature of the peat layer is not evenly distributed. Lateral variation within the peat layer is also noted in the electrical imaging pseudo-sections. This implies that there is a difference in the composition within the peat layer, which might related to the moisture content distribution of the dyke or from the geologic history of the area, it might be interrupted lenses with low resistivity.

Based on this analysis, some similarities were noted between the high resistivity and the low radiation temperature as well as between low resistivity and high radiation values (section 1 and

Figure 2). Differences were also observed especially in their lateral variation. Their lateral variations did not relate to each other. This is because in both techniques, it is difficult to differentiate the compositional variation from the variation due to moisture content or other factors. This can be related to the geotechnical properties of the unconsolidated soils that can vary over a small distance. For instance, the distribution of water content and total unit weight of a peat layer varies in all directions (vertically and horizontally). The variations perpendicular to the survey line are not separately indicated by the 2-D electrical imaging survey. This is because the 2-D electrical imaging survey gives an apparent 2D section of the variation of the resistivity, but in reality measures the resistivity over a volume, thus also including variations perpendicular to the section. On the other hand, the TIR images have shallow information of the surface (50-100cm). However, the separation distance between these images ranges from 1m at the top to 9m at the bottom part of the dyke (Figure 1). The grass that covers the dyke material has its own influence on the result of the thermal radiation. The presence of the grass minimizes the possible interaction between the topsoil of the dyke and the solar radiation. This implies that exposed dyke materials react to the solar radiation and atmospheric temperature quicker. For example, in Figure 2 of the thermal image the dark spots inside the circle are referred to the exposed topsoil of the dyke and have higher temperature than the surrounding soil materials, which are covered by the grass. While the electrical imaging surveys record, represent only the reading comes from the dyke materials.

1.2 Relationship between TIR and NIR

The above correlation between the TIR images and the 2-D electrical imaging indicates the general variation in the composition of the dyke materials. Therefore, this section will try to establish the correlation between TIR and NIR images to derive supplementary information that can strengthen the above correlation. According to the Kirchhoff's radiation law, when reflectivity increases the absorbance will decrease and vice-verse. This implies that the NIR and TIR can have an inverse relationship. This is true for the images that are acquired in similar wavelength propagation. However, in this study the wavelength propagation of NIR (0.52 to 0.95 µm) is different from that of TIR (8 to 14 µm). Therefore, the relationship may not fulfill the above law.

1.2.1 VREESTERDIJK

The trend of the relationship is not clearly illustrated for images of summer (Figure 5a) and winter (Figure 5c). Many pixel values are concentrated in the middle of the plot. Some extreme values are scattered in all direction. In both plots for high temperature value, there are high as well as low reflectance values in the plot. This can imply that the thermal images are not only the emitted temperature results from the grass but also the emitted temperature of the topsoil. The relation between the TIR and NIR of October has relatively negative trend. The radiation temperature decreases as the reflectance DN-values of the NIR increases (Figure 5b). This is because in the TIR image the radiation temperature is high for the exposed topsoil part of the dyke and relatively low for areas covered by grass (Figure 6). While the reflectance in the NIR is high for areas with the presence of green grasses and low for the exposed topsoil (Appendix I, Figure 11). This makes the images to show negative correlation not due to the variation in the composition of the dyke. Some sample points show a positive relation in the left lower corner of the scatter plot between the radiation temperature and reflectance value of October.

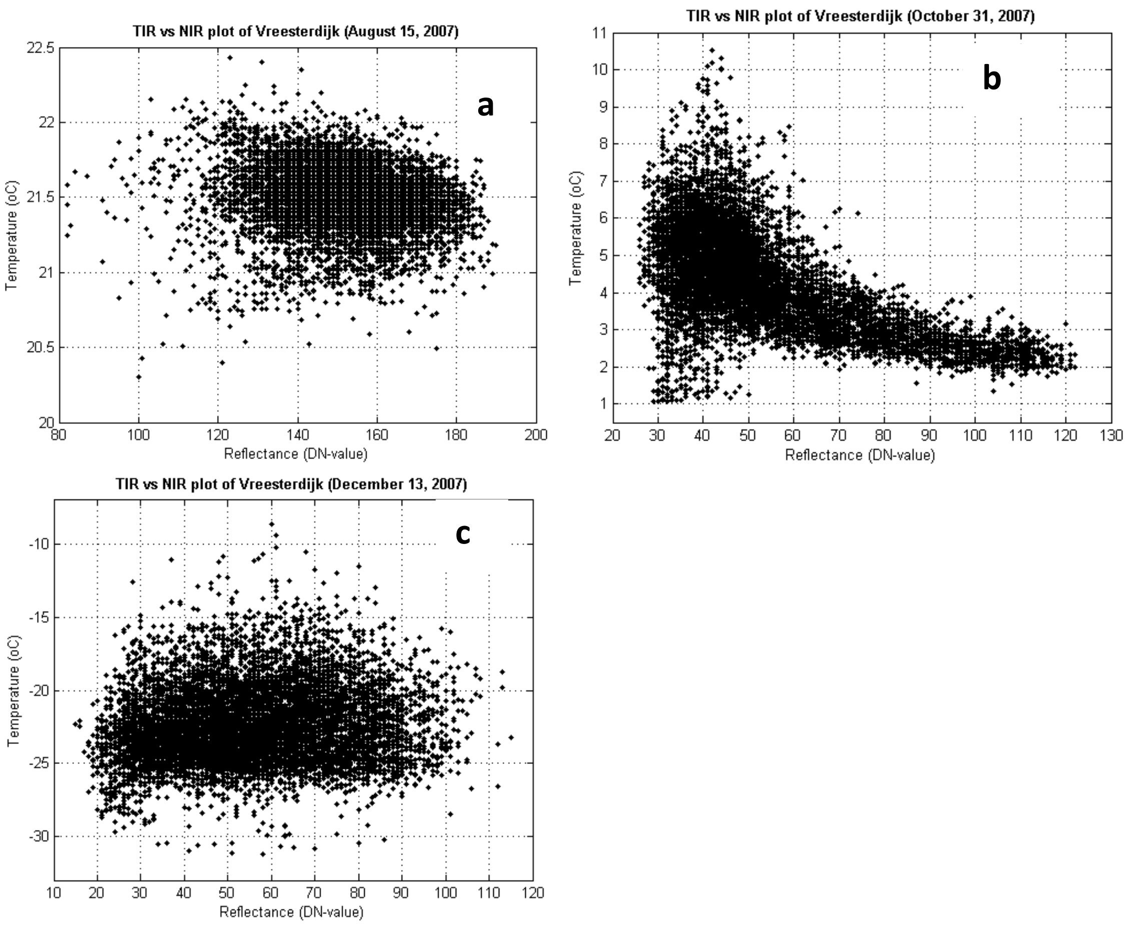

Figure 5. The scatter plot shows the possible correlation between images of TIR and NIR of Vreesterdijk in (a) August, (b) October and (c) December field campaigns

1.2.2 TEMPELDIJK-NORTH

For the images of summer, the range of values for the reflectance in the near infrared is about 100 (100 - 200) in DN-value while the difference in the radiation temperature of the dyke materials is 2^{o}C. Thus, most part of the radiation temperature shows the same value for the higher and lower reflectance value. The scatter plot between these images does not show a possible trend of correlation (Figure 6). In the upper right corner of the plot it shows a positive relation while the extreme sample points in the upper left and lower right corner show a possibly negative relation. However many of the sample points are concentrated in the centre of the plot. Similarly, the scatter plot of October shows the same result as the summer. Many sample points are concentrating by forming a circle cluster in the centre of the plot. The pot of December is different from the other plots. Ths is probably due to the sun angle difference. The pixels with the maximum reflectance DN-values (up to 255) are due to the grass, which were exposed to the sun light. For the same radiation temperature value, there are different reflectance values. For example for -28^{o}C radiation temperature value, the corresponding reflectance value ranges from 50 up to 255 DN-values. This indicates the effect of the shadow on both infrared images. More over it is highly influenced the NIR images that affect the reflectance of the grass (appendix I, Figure 12lower).

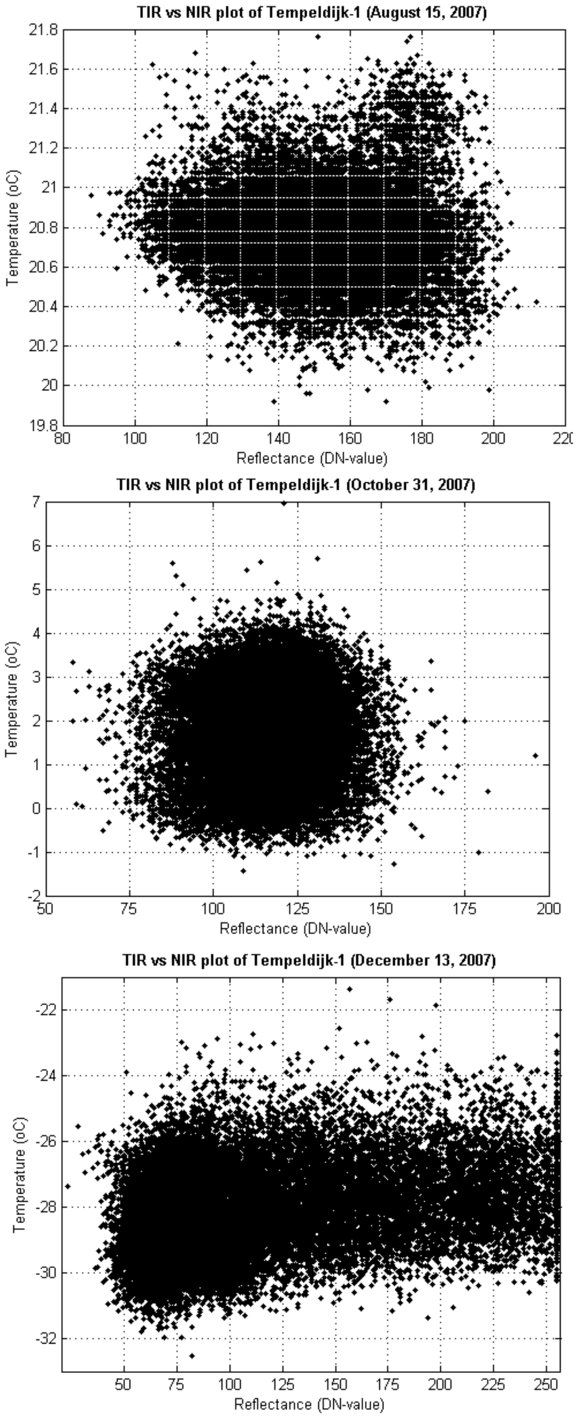

Figure 6. The scatter plot shows the possible correlation between images of TIR and NIR of Tempeldijk-North in (a) August (b) October and (c) December field campaigns (Tempeldijk-1 is Tempeldijk-North).

1.2.3 TEMPELDIJK-SOUTH

The scatter plots between these images of Tempeldijk-South do not have any indication of correlation. The extreme sample points are scatter in every direction of the plot (Figure 7).

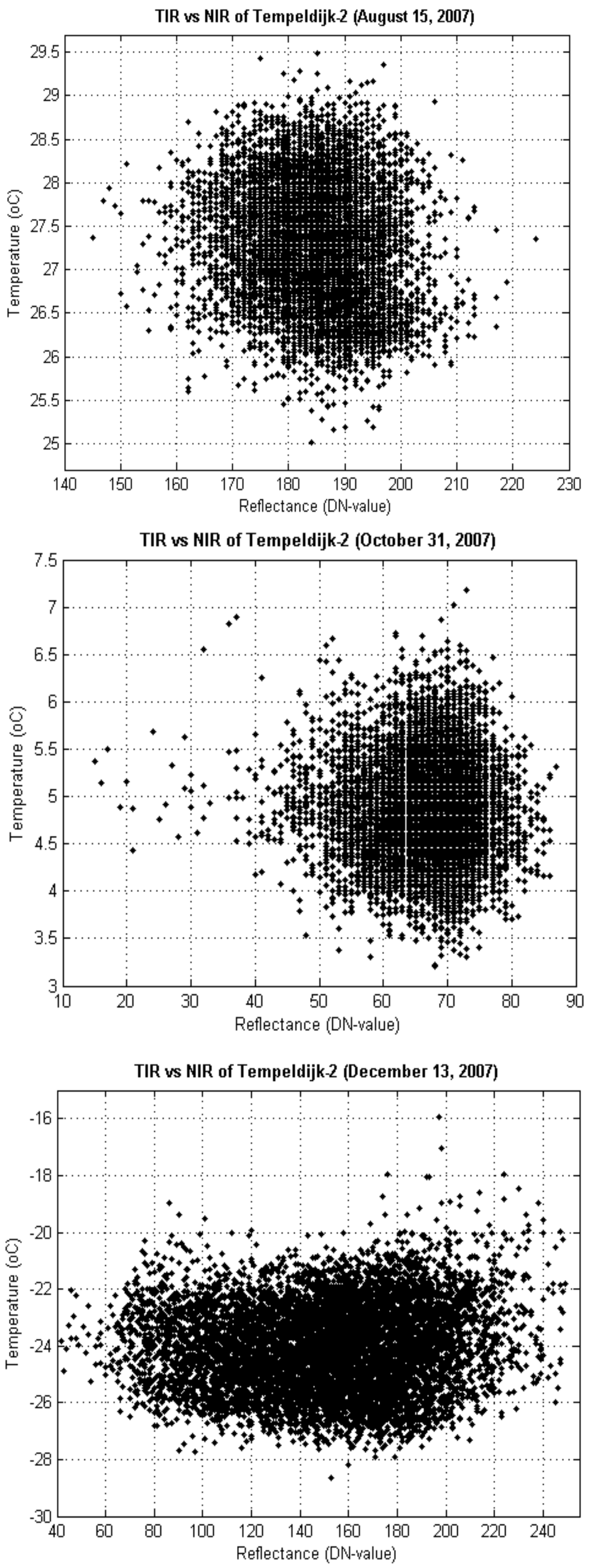

Figure 7: the scatter plot shows the possible correlation between images of TIR and NIR of Tempeldijk-2 in (a) August, (b) October and (c) December field campaigns (Tempeldijk-2 is Tempeldijk-South)